EARTH SURFACE PROCESSES AND LANDFORMS
Earth Surf. Process. Landforms **38**, 1838–1850 (2013)

Published online 5 May 2013 in Wiley Online Library
(wileyonlinelibrary.com) DOI: 10.1002/esp.3427

Schmidt hammer exposure-age dating (SHD) of late Quaternary fluvial terraces in New Zealand

Timothy Stahl,[1]* Stefan Winkler,[1] Mark Quigley,[1] Mark Bebbington,[2] Brendan Duffy[1] and Daniel Duke[1]
[1] Department of Geological Sciences, University of Canterbury, Christchurch, New Zealand
[2] Volcanic Risk Solutions, Massey University, Palmerston North, New Zealand

Received 26 May 2012; Revised 6 December 2012; Accepted 21 March 2013

*Correspondence to: Timothy Stahl, Department of Geological Sciences, University of Canterbury, Christchurch, New Zealand. E-mail: timothy.stahl@pg.canterbury.ac.nz

ESPL
Earth Surface Processes and Landforms

ABSTRACT: Schmidt hammer (SH) *R*-values are reported for surface clasts from numerically dated Holocene and Pleistocene fluvial terraces in the South Island of New Zealand. The *R*-values are combined with previously obtained weathering rind, radiocarbon, terrestrial cosmogenic nuclide and luminescence terrace ages to derive SH *R*-value chronofunctions for greywacke clasts from four distinct locations. Our results show that different weathering rates affect the form of the SH *R*-value versus Age curve, however a fundamental dependency between the two remains constant over timescales ranging from 10^2 to 10^5 years. Power law scaling constants suggest changes in clast weathering rates are primarily affected by climatic (precipitation and temperature) and sedimentologic variables (source terrane petrology). Age uncertainties of ~22% of the surface age suggest that Schmidt hammer exposure-age dating (SHD) is a reliable calibrated-age dating technique for fluvial terraces. Copyright © 2013 John Wiley & Sons, Ltd.

KEYWORDS: Schmidt hammer; exposure-age dating; fluvial terrace; outwash plain

Introduction

Geomorphic studies frequently utilize age dating of fluvial terraces and glacial outwash plains (e.g. Bull and Knuepfer, 1987; Molnar *et al.*, 1994; Amos *et al.*, 2007, 2010; Barrell *et al.*, 2011). Isotopic and radiogenic techniques have the ability to provide numerical ages but are typically expensive and labour intensive. River deposits that lack suitable organic material for radiocarbon dating, have complex mixing, burial and/or exposure histories that complicate terrestrial cosmogenic nuclide dating (TCND) or contain detritus that was not completely 'bleached' prior to deposition for luminescence dating, may be challenging to date using these techniques.

Clasts exposed at or near the surface weather by chemical, physical and biological processes that collectively reduce the mechanical strength of the rock (e.g. Birkeland and Noller, 2000; Walker, 2005). Time-dependent variables like rock weathering rind thickness (e.g. Chinn, 1981; Knuepfer, 1988; McSaveney, 1992; Oguchi and Matsukura, 1999; Laustela *et al.*, 2003), surface roughness (e.g. Benedict, 1985), P-wave velocity (Crook and Gillespie, 1986) and clast density (Maizels, 1989) may be used to derive relative-ages for populations of surface clasts. The weathering-induced reduction of rock strength can also be measured using the Schmidt hammer (SH).

The SH was originally developed for concrete testing but has been widely used as a field test of rock hardness and relative-dating technique for over three decades (Schmidt, 1951; Day and Goudie, 1977; Day, 1980; Matthews and Shakesby, 1984; McCarroll, 1991a, 1994; Goudie, 2006; Shakesby *et al.*, 2006, 2011). SH rebound value (*R*-value) tests rock hardness at the surface by measuring the percentage rebound of a hammer mass in a controlled impact against the test surface (Goudie, 2006; Shakesby *et al.*, 2006). A number of workers have shown that decreasing SH *R*-values, and thus a decrease in rock mechanical strength, correspond with an increase in rock surface exposure age (e.g. Matthews and Shakesby, 1984; McCarroll, 1989, 1991b, 1991c; Winkler, 2005; Shakesby *et al.*, 2006, 2011; Matthews and Winkler, 2011).

A geomorphic feature with independent, numerical age control can be used to quantify the relationship between SH *R*-values and exposure age. The *R*-values of a population of surface clasts reflect the time-dependent mechanical degradation of the rock, and thus an approximate time since a presently stable surface was abandoned following erosion or aggradation. If numerical ages exist for a sequence of two or more features, then a chronofunction that relates SH *R*-values to surface exposure ages may be derived and used to estimate the surface ages for other undated deposits within the sequence (Shakesby *et al.*, 2006; Winkler, 2009; Matthews and Owen, 2010). Geomorphic studies coupled with SH analyses have been used to produce calibrated-age curves for glacial, peri-glacial, mass movement, and alluvial fan deposits (e.g. McCarroll, 1991a; Nesje *et al.*, 1994a, 1994b; White *et al.*, 1998; Aa *et al.*, 2007; Kellerer-Pirklbauer *et al.*, 2008; Rode and Kellerer-Pirklbauer, 2011; Shakesby *et al.*, 2011), and polished bedrock surfaces (e.g. Gupta *et al.*, 2009; Matthews and Owen, 2010).

Previous studies have yielded strong correlations between average SH *R*-values and surface exposure ages within the Holocene (McCarroll, 1987; Nicholas and Butler, 1996; Winkler, 2005; Matthews and Owen, 2010; Shakesby *et al.*, 2011). Only a few studies have applied SH exposure-age dating (SHD) to pre-Holocene surfaces, with variable results (e.g. White *et al.*, 1998;

Engel, 2007; Sánchez *et al.*, 2009). Shakesby *et al.* (2006) and White *et al.* (1998) are the only studies to apply SHD to fluvial deposits.

Fresh, fluvially-polished rock tends to yield the highest *R*-values for any given lithology (Ericson, 2004; Gupta *et al.*, 2009) and rounded clasts have the highest *R*-values of all sediment morphologies (McCarroll, 1989; Shakesby *et al.*, 2006), possibly as a result of minimal surface roughness (Williams and Robinson, 1983; McCarroll, 1989). Given the relatively high initial strength and low initial surface roughness of the lithologies and clasts present in New Zealand's fluvial terraces (Read *et al.*, 1999), SHD may be useful over a longer (pre-Holocene) timescale than commonly attempted.

In this paper, SHD is applied to surface clasts on fluvial terraces for the first time. SH analyses are combined with published luminescence, radiocarbon, weathering rind and TCND ages to construct age-calibration curves for a suite of terraces in New Zealand's South Island. Climatic and petrologic data are used to compare weathering rates between study sites and predict chronofunction parameters.

Study Sites

The four study sites in the central South Island of New Zealand (Figure 1A and 1B) were chosen because they contain well-dated Holocene and Pleistocene terraces, have similar clast lithologies and they span a range of contemporary climates. The ages used to calibrate SHD in this study are the best estimates of abandonment ages for the terraces. Terraces formed by lateral incision into pre-existing fan deposits, without subsequent aggradation or leaving a veneer of gravel prior to abandonment, may yield exposure ages older than the

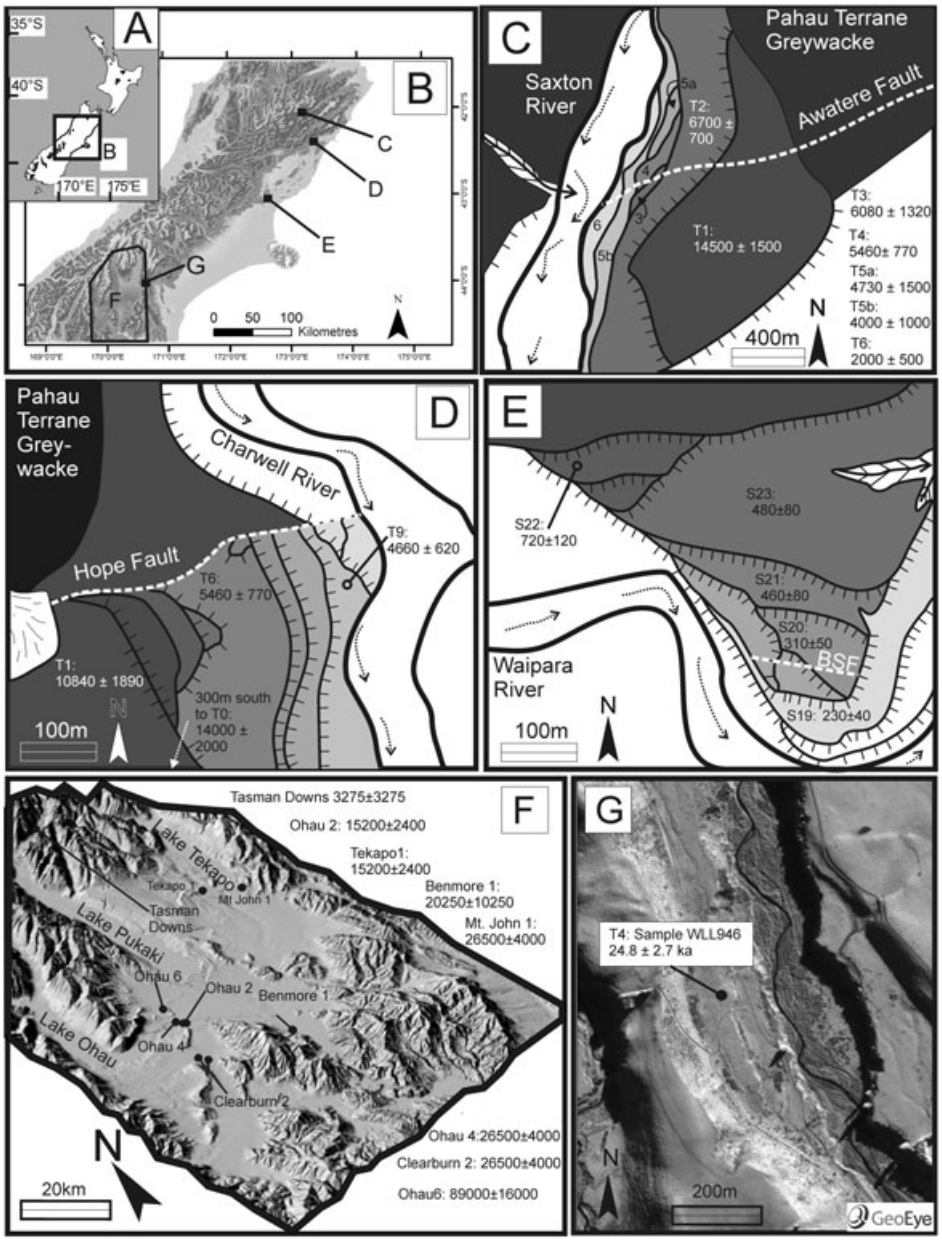

Figure 1. Location map of study sites around South Island, New Zealand (A and B) and generalized geomorphic maps of study sites. All ages are given in years unless otherwise specified. (C) Saxton River terraces (modified after Mason *et al.*, 2006); (D) Charwell River terraces (modified after Knuepfer, 1984); (E) Waipara River terraces (modified after Nicol and Campbell, 2001); (F) 15 m digital elevation model (3× vertical exaggeration) of the Mackenzie basin and sites selected for sampling; (G) *GeoEye* aerial imagery of the Cloudy Peaks test site, showing location of optically stimulated luminescence (OSL) sample and paired fluvial terraces incised by stream flowing north-south (N-S) in image. References for ages in C–G and Schmidt hammer data are given in Table I.

abandonment of the terrace tread (i.e. skewed to the age of deposition of the fan gravel). Weathering rind exposure-ages for terrace treads, as well as local terrace stratigraphy, suggest episodes of minor aggradation prior to abandonment for all of the terraces in this study (e.g. Bull, 1990).

The Saxton River terraces (Figure 1C) have been extensively studied in attempts to calculate slip rates on the cross-cutting Awatere Fault (Knuepfer, 1988; McCalpin, 1996; Mason *et al.*, 2006). The site consists of six, previously mapped terraces incised into a late Pleistocene (~16 ka) fan. For the purposes of our investigation, we differentiated between two terraces (T5a and T5b), previously mapped as T5, and separated by a ~1 m riser. This was done to test the resolution of the SH in distinguishing between terraces formed in a short-time period. All of the terraces except for T3 and T5a have been previously dated using weathering rinds, which produce consistently reliable results in New Zealand's well-indurated Torlesse greywacke (Chinn, 1981; Whitehouse *et al.*, 1986; Knuepfer, 1984, 1988; McSaveney, 1992; Nicol and Campbell, 2001). Ages were inferred for terraces where maximum and minimum age control was available from adjacent terraces.

Weathering rind ages are used in conjunction with numerical dating. McCalpin (1996) obtained a radiocarbon age of 1186 ± 110 years BP (2012) within the Saxton T6 terrace overbank silts. This minimum age of abandonment for the terrace tread is younger than but consistent with Knuepfer's (1988) weathering rind age of 2000 ± 500 years for abandonment of T6, which is adopted in this study. Mason *et al.* (2006) have extensively dated the oldest terraces T1 and T2 with multiple radiocarbon and optically stimulated luminescence (OSL) dates. Their preferred age of T1 terrace abandonment was an OSL age of $14\ 500 \pm 1500$ years derived from fluvial silts capping the terrace gravels. A discrepancy between Mason *et al.*'s (2006) OSL age for T1 (see Figure 1) and a younger weathering rind age (9410 ± 1570 years; Knuepfer, 1988) was attributed to deflation of a silt cover that previously covered the exposed gravel (Mason *et al.*, 2006). This was interpreted to have reduced the surface exposure time and hence the weathering rind age. We therefore use Mason *et al.*'s (2006) OSL ages for the abandonment of T1 and T2 in this analysis as the best estimate of true surface age.

The Charwell River study site consists of a flight of 12 post-14 ka terraces along the Hope Fault-bounded range front (Figure 1D). The terraces were formed by incision into late Pleistocene gravel and greywacke bedrock, and are capped with a veneer of younger aggradational gravels (Bull and Knuepfer, 1987). The oldest and highest surface was not mapped by Knuepfer (1984) and we assume this surface, named here as T0 to keep consistent terminology, is the apex of the 14 ka aggradation event described by Bull and Knuepfer (1987). Terraces younger than T0 were dated by Knuepfer (1988) using weathering rinds calibrated with radiocarbon and with other studies. Of these 11, three were selected for SHD – most terraces were only subtly preserved in the landscape and lacked surface clasts. Although predominantly Torlesse greywacke (Pahau sub-terrane), the modern stream also contains boulders of trachybasalt, either from the local Gridiron/Lookout Formations (Suggate, 1958; Challis, 1966) or from an unmapped volcanic member of the Torlesse greywacke. The weathering pattern of both lithologies is similar in surface clasts on abandoned terraces with the trachybasalt representing a relatively low proportion of the total clast count.

The Waipara River study site consists of between five cut-in-fill terraces that are all younger than 1 ka and are displaced by the Bobys Stream Fault ('BSF' in Figure 1E) (Nicol and Campbell, 2001; Campbell *et al.*, 2003). The terraces consist primarily of a Torlesse greywacke gravel veneer (undifferentiated Pahau and Esk Head Melange sub-terranes) overlying a late Pleistocene outwash gravel strath surface. Nicol and Campbell (2001) used weathering rinds to date five of the terraces on site, as well as several others in the area with reliable results. Locally derived clasts of coarse-grained, Tertiary sandstone were identified on the three oldest terraces. On younger terraces and in the modern stream, coarse limestone boulders were readily identifiable. Some greywacke surface clasts on these terraces were coated with a calcium-carbonate film from the weathering limestone.

The Mackenzie basin is an intermontane basin located in the central South Island (Figure 1F). The study sites are dispersed across the basin where low relief moraines, glacial lakes, and glaciofluvial outwash plains predominate. Glacial and periglacial features have been numerically dated using various techniques including OSL and TSL (thermally stimulated luminescence), TCND, and radiocarbon (Barrell and Cox, 2003; Amos *et al.*, 2007, 2010; Schaefer *et al.*, 2009; Barrell, 2011; Barrell *et al.*, 2011). The ages of these features range from the 'Little Ice Age' to at least 100–150 ka. Outwash plains are exceptionally preserved due to the dry climate and distance from the Main Divide, which allows reliable mapping of correlative deposits and features (e.g. Maizels, 1989; Amos *et al.*, 2007, 2010; Barrell *et al.*, 2011). Surface clasts are all Torlesse greywacke (Rakaia sub-terrane). Outwash plains in this study fall into five categories based on numerical ages: marine isotope stage (MIS) 5 or 6 (89 ± 16 ka); early MIS 2 ($26 \cdot 5 \pm 4$ ka); mid MIS 2 (inferred as $20 \cdot 25 \pm 10 \cdot 25$ ka); late MIS 2 ($15 \cdot 2 \pm 2 \cdot 3$ ka); and Holocene ($3 \cdot 275 \pm 3 \cdot 275$ ka) (Figure 1F). Efforts were taken to sample where previously numerically dated samples had been taken; however, some samples were taken in locations of unknown age that have been mapped and correlated with dated units elsewhere (Amos *et al.*, 2007, 2010; Barrell *et al.*, 2011). Where minimum or maximum numerical ages were obtained, the age and error inferred for the surface was conservatively set midway between bounding units/surfaces of known age (Table I). In addition to these four study sites, a test site at Cloudy Peaks, on the edge of the Mackenzie basin, was selected for comparison between OSL and SHD techniques. An OSL age of $24 \cdot 8 \pm 2 \cdot 7$ ka (Figure 1G; Table II) was obtained from fluvial silts overlying river gravel in a terrace located approximately 40 m above stream level. Surface clasts used for SHD consist of Rakaia sub-terrane greywacke rocks.

Methodology

An N-type SH (SH_N) with a calibrated impact energy of $2 \cdot 207$ N m (Proceq SA, 2004) was used in this study. Control of potential instrument error was constrained by pre- and post-sampling checks of correct calibration using a test anvil in order to detect instrumental deterioration during the measurement campaign. One SH impact was delivered on each clast for a minimum of 50 clasts per surface (e.g. Matthews and Shakesby, 1984; Winkler, 2005). This provides a statistically significant sample size and produces similar results to much larger sample sizes (Niedzielski *et al.*, 2009). Although recently developed test designs with multiple sub-samples and an overall largely increased number of clasts measured at one site can significantly tighten the instrumental error margins (e.g. Shakesby *et al.*, 2011; Matthews and Winkler, 2011), the restricted availability of clasts suitable for testing and the character of our test sites preclude such attempts.

Where possible, two independent sets of 50 clasts were sampled on each surface to test for data consistency, as has been suggested for weathering rind studies (McSaveney, 1992). A third test, during which the SH_N operator was selective to sample only

Table I. Terrace names by study site, the amount of SH measurements (n) taken, SH_N mean/median values and references for terrace ages given in Figure 1

Site	SH_N mean	SH_N median (SH_R)	Reference for numerical age given in Figure 1
Saxton River			
T1 ($n=150$)	39·0	38	Mason *et al*. (2006)
T2 ($n=100$)	40·6	40·5	Mason *et al*. (2006)
T3 ($n=50$)	43·3	44	Inferred from Mason *et al*. (2006) and Knuepfer (1988)
T4 ($n=100$)	43·2	43	Knuepfer (1988)
T5a ($n=100$)	45·6	47	Inferred from Knuepfer (1988)
T5b ($n=100$)	47·0	48	Knuepfer (1988)
T6 ($n=50$)	51·3	52	Knuepfer (1988) and McCalpin (1996)
Modern ($n=50$)	60·9	61·5	
Charwell River			
T0 ($n=50$)	33·9	33	Bull and Knuepfer (1987)
T1 ($n=100$)	35·1	35	Knuepfer (1988)
T6 ($n=50$)	39·1	38	Knuepfer (1988)
T9 ($n=100$)	42·9	44	Knuepfer (1988)
Modern ($n=50$)	56·0	55·5	
Waipara River			
S22 ($n=50$)	44·0	44	Nicol and Campbell (2001)
S23 ($n=100$)	46·1	45·5	Nicol and Campbell (2001)
S21 ($n=50$)	47·4	47·5	Nicol and Campbell (2001)
S20 ($n=50$)	49·3	48·5	Nicol and Campbell (2001)
S19 ($n=50$)	54·2	55	Nicol and Campbell (2001)
Modern ($n=50$)	60·9	62	
Mackenzie basin			
Tekapo1 ($n=100$)	46·0	46	Amos *et al*. (2007, 2010) and Barrell *et al*. (2011)
Benmore1 ($n=100$)	45·2	45·5	Inferred from Barrell and Cox (2003)
Ohau2 ($n=100$)	46·5	47	Amos *et al*. (2007, 2010)
Ohau4 ($n=100$)	42·3	41·5	Amos *et al*. (2007, 2010)
Mt John1 ($n=100$)	41·5	42	Amos *et al*. (2007, 2010) and Barrell *et al*. (2011)
Clearburn1 ($n=100$)	40·2	39·5	Amos *et al*. (2007, 2010) and Barrell *et al*. (2011)
Ohau6 ($n=50$)	31·7	31·5	Amos *et al*. (2007, 2010)
Tasman Downs ($n=50$)	58·0	60	Inferred from Schaefer *et al*. (2009)
Modern ($n=50$)	60·2	62	
Cloudy peaks			
T4	39	40·13	This study

Table II. Optically stimulated luminescence results for T4 at the Cloudy Peaks test site- measured *a*-value, equivalent dose, cosmic doserate, total doserate, and OSL age

Sample[a]	*a* Value	D_e[b] (Gyr)	dD_c/dt[c] (Gyr/ka)	dD/dt[d]	OSL age (ka)	Field code
WLL946	0·05 ±0·01	88·74 ± 8·70	0·2162 ± 0·0108	3·57 ± 0·17	24·8 ± 2·7	T49611

[a]Sample preparation and measurements performed at the School of Earth Sciences, Victoria University of Wellington, Wellington, New Zealand.
[b]Equivalent dose.
[c]Contribution of cosmic radiation to the total doserate.
[d]Total doserate.

clasts with geomorphic stability indicators (i.e. rock varnish, raised quartz veins, lichen cover), was conducted in instances where the surrounding geomorphology visibly suggested reworking or secondary deposition (e.g. T1 at the Saxton River site). This method weighted the dataset towards clasts with a more reliable exposure history without discarding data that may be relevant to the surface exposure age.

To avoid the effects of rock moisture content (Sumner and Nel, 2002) and instrumental inconsistencies due to humidity causing corrosion/rust inside the SH, sampling was carried out in dry conditions. The clast surfaces were not brushed clean or smoothed prior to SH sampling so that the full weathering rind and clast surface roughness were preserved. The sampled surfaces were lichen free and any obvious mineral veins or structural discontinuities were avoided (Ozbek and Gul, 2011). The SH was held as vertically as possible on horizontal to sub-horizontal clast surfaces to avoid biased *R*-values created by varying impact angles and protruding mineral grains on rebound (André, 1996; Ericson, 2004; Shakesby *et al*., 2011; Proceq, 2004). If small particles were chipped off during sampling or the sound of the SH impact was not resonant (indicating possible cracks invisible below the surface), an additional attempt was made to resample the clast surface from another impact point. If the same problem was encountered, the clast was omitted from the dataset.

Clasts with less than 15 cm of rock exposed at the surface were avoided during sampling. Although ideally larger clasts/boulders are preferred with SH studies, the availability of clast prevented us from increasing this minimum size. While there is little constraint on subsurface clast geometry and edge effects in clasts of this size in the present study, we consider the

chosen minimum of 15 cm exposed rock reasonable on the following bases:

(i) Demirdag *et al*. (2009) showed in a series of tests that rocks from various lithologies with a minimum edge dimension greater than 11 cm yield consistent L-type SH *R*-values. The L-type SH has a lower impact energy than the SH_N, and thus the minimum edge dimension required for consistent results is likely somewhat higher for a SH_N. Nevertheless, the present cut off value of 15 cm is larger than suggested by Aydin (2009) for International Society of Rock Mechanics standards (100 mm at the point of impact for SH_N), and equivalent to those suggested in the ASTM (2005) (minimum 15 cm).
(ii) The terrace gravels we observed in outcrop rarely contained disk-shaped or 'platy' clasts, which typically have much smaller edge dimensions than required for sampling.
(iii) Every boulder was kicked before sampling to check for stability, and clasts that moved during sampling were considered unsuitable. Additionally, if a clast was chipped during sampling, or the SH sounded flat rather than resonant, indicative of a shallow discontinuity (as with disk-shaped clasts), the *R*-value was omitted from the dataset.
(iv) Some of the impact energy during sampling may have been dissipated within the underlying soil as opposed to wholly within/on the clast being sampled. We believe that these effects were minimal, as most clasts sampled were firmly encased in soil. So long as the effect is constant (i.e. the average clast size and mechanical soil properties remain unchanged from site to site) our results should be internally consistent.
(v) The SH_N was chosen over devices with less impact energy (e.g. Equotip) due to significantly smaller *R*-value variance (Viles *et al*., 2011) and a much more frequent usage in geomorphology in both New Zealand and elsewhere.

When different lithologies could be identified in the terraces and active stream bed (e.g. the Waipara River), care was taken to sample only the Torlesse greywacke. Where the weathering of two similar lithologies on older terraces made identification of Torlesse greywacke difficult (such as volcanic rocks in the Charwell River), both lithologies were sampled in the modern stream. Catchment lithologies and proportional contributions to the fluvial system are assumed not to have changed over time.

For surface clasts with a simple exposure history, SH *R*-values are expected to be normally distributed (Winkler, 2005, 2009) and the mean *R*-value from a series of measurements is the most often used proxy for the surface exposure age (e.g. Goudie, 2006). In this study, slight differences were sometimes observed in the individual *R*-value distributions and dataset means when comparing individual tests on the same surface ($n = 50$ per test) to each other and/or the combined dataset. Niedzielski *et al*. (2009) found that using the median increased *R*-value consistency and reduced the required sample size for a range of rock types. The median *R*-value (SH_R) is less affected by statistical outliers than the mean and is preferred in this study. Both mean and median values for the study sites are listed in Table I.

A Kruskal–Wallis analysis of variance (ANOVA) test (Kruskal and Wallis, 1952) was used to test for significant differences among SH_R. The analysis was run as a multiple comparisons test (comparing each median to every other median) at the 1σ level using a Dunn–Sidak correction (Sidak, 1967). This is a much more conservative approach than identifying significant differences in a dataset *sensu stricto*, but less conservative than multiple comparison tests with other adjustment techniques (e.g. Abdi, 2007).

Age-SH_R correlations are derived for the Saxton River terraces (Figure 1C), Charwell River terraces (Figure 1D), Waipara River terraces (Figure 1E), and Mackenzie basin outwash plains (Figure 1F), with published age errors and 95% standard errors reported for age and SH_R, respectively.

Climate data for our study sites were compiled along with petrologic information from Torlesse greywacke sub-terranes (Table III). This was done to investigate possible changes in weathering rates due to differences in precipitation, temperature, and source rock composition. Maximum temperature (in °C) and precipitation data (in millimetres) were downloaded from the National Institute of Water and Atmospheric (NIWA) Research's CliFlo database as monthly averages over a 30-year time period. Climate stations that were nearest to our study sites (maximum 55 km) and in similar microclimates were chosen. For the Charwell River, Saxton River, and Cloudy Peaks sites, temperatures were adjusted using an average NZ lapse rate of 0·5 °C/100 m (Norton, 1985). Thirty-year averages for each month were extrapolated to full year values (i.e. multiplied by 12) to obtain a range of possible annual precipitations (MAP_{month}) and maximum mean temperatures (MAT_{month}). These are preferred over mean annual temperature and precipitation because the latter give no indication of climate fluctuations sub-annually. More importantly, the exponential dependence of chemical weathering rates on temperature illustrates that climate extremes control long-term rates more so than lower average values (e.g. Velbel, 1990).

Petrologic data for the Torlesse sub-terranes were compiled from a variety of sources and are reported as Quartz-Feldspar-Lithics (QFL) modal percentages (Table III). For the Rakaia sub-terrane, averages were calculated from MacKinnon's (1983) Petrofacies 1 through 4. The modal percentages of Petrofacies 5 (MacKinnon, 1983; Roser and Korsch, 1999) were used for the Pahau terrane, and supported by Barnes' (1990) data. QFL percentages from greywacke within the Esk Head Melange are more difficult to quantify, but data from the greywacke blocks in the melange proper (Botsford, 1983) and gradational contact into the Pahau terrane (Feary, 1979) were taken as representative modal percentages.

Results

SH data

SH_R values for all study sites decrease with an increase in terrace age (Figure 2). In all three curves, SH_R can be correlated with age using a power law function of the simple form

$$SH_R = a * (age)^b \quad (1)$$

where a and b are statistically estimated constants (Figure 2A–2C). The power law describes the SH_R–age relationship over timescales ranging from 10^2 years (Waipara) to 10^5 years (Mackenzie basin) timescales. The curves are generally defined by a rapid decrease in SH_R values from clasts within the modern stream to clasts in the youngest terrace, followed by conformity to the power law (Equation 1). This implies that a short period (*c*. 10^2–10^3 years for the study sites considered herein) of relatively rapid weathering occurs during and/or after the transfer of alluvium from an active channel into an 'inactive' terrace.

To test if the curves have a common slope, we used the statistical package (S)MATR and fit curves with a Major Axis (MA) regression (see Warton *et al*., 2006, for a full review). This

Table III. Thirty-year monthly averages of maximum temperature (in °C) and precipitation (in millimetres) extrapolated for a full year (MAT_{month} and MAP_{month}, respectively)

Site	Climate station	Distance to study site	Elevation difference	MAT_{Jan}	MAP_{Jan}	MAT_{Feb}	MAP_{Feb}	MAT_{Mar}	MAP_{Mar}	MAT_{Apr}	MAP_{Apr}	MAT_{May}	MAP_{May}	MAT_{Jun}	MAP_{Jun}	MAT_{Jul}
Saxton	Molesworth	9 km	+ 70 m	21	521	20·9	548	18·5	586	15·1	572	11·5	649	8·0	706	6·6
Charwell	Kaikoura Aws	28 km	+ 300 m	18·9	468	18·5	622	17·2	710	14·7	666	12·7	679	10·5	900	9·4
Waipara	Waipara West	3 km	0	23·8	691	23·7	491	21·6	544	19	672	15·6	434	12·8	635	12
Mackenzie	Lake Tekapo, Air Safaris	Variable; <55 km	Variable, not adjusted	21·6	624	21·3	396	18·8	564	14·9	672	10·7	720	7	600	5·8
Cloudy Peaks	Fairlie	14 km	+ 200 m	20·6	708	20·4	564	18·6	888	15·7	624	11·9	852	9·3	540	8·3

Site	MAP_{Jul}	MAT_{Aug}	MAP_{Aug}	MAT_{Sep}	MAP_{Sep}	MAT_{Oct}	MAP_{Oct}	MAT_{Nov}	MAP_{Nov}	MAT_{Dec}	MAP_{Dec}	Sub-terrane	Q	F	L
Saxton	649	8·3	574	11·4	634	13·5	830	15·8	595	18·4	695	Pahau	0·26	0·34	0·40
Charwell	1103	10·2	803	12·2	682	13·8	757	15·5	703	17·6	563	Pahau	0·26	0·34	0·40
Waipara	646	13·4	755	15·8	756	17·7	472	19·8	719	22·1	628	Pahau/Esk Head	0·40	0·20	0·40
Mackenzie	624	8·2	648	11·9	636	14·5	612	17·2	624	19·4	576	Rakaia	0·30	0·50	0·20
Cloudy Peaks	612	10	588	13·3	528	15·5	756	17·4	720	19·1	804	Rakaia	0·30	0·50	0·20

Note: The data range is from 1981 to 2010, except for Cloudy Peaks site/Fairlie weather station, where the only available data range was from 1951 to 1980. Petrologic data are given as modal proportions of Quartz-Feldspar-Lithics (QFL) for Torlesse greywacke sub-terranes.

was chosen in place of ordinary least squares (OLS) fitting for the following reasons:

(i) MA fitting uses a maximum likelihood estimation (MLE) of slope when deriving a common slope among different groups (e.g. different study sites). Using a MLE reduces Type 1 error (rejection of a potentially true hypothesis of common slope) and does not assume constant SH_R variance with age (homoscedasticity) (Warton *et al.*, 2006; Shakesby *et al.*, 2011). This enables comparison of terraces spanning three orders of magnitude of ages and errors.

(ii) MA fitting accounts for uncertainty in numerical age as well as SH_R. An MA fitted line optimizes residuals perpendicular from the curve at the data point, as opposed to solely in the y (SH_R) direction.

(iii) MA is better suited to describing theoretical relationships between two variables; OLS is more appropriate when the goal is to predict y from x (Warton *et al.*, 2006). The interest in this study is the former.

(iv) In this study, MA yields values that generally agree with, but lie between the extremes of, OLS and standardized major axis fitting (Warton *et al.*, 2006).

A common slope (b-value in Equation 1) of –0·189 was determined with high statistical significance ($p = 0 \cdot 678 > 0 \cdot 05$). The a-value of each curve was then computed using non-linear least squares with the fixed, common b-value. Table IV shows the results of these tests and curve fitting. The a-value for the Cloudy Peaks test site was determined by rearranging Equation 1 ($a = 264$).

The power law constants control different aspects of the chronofunction form. The a-value, or scaling constant, controls the 'position' of the SH_R-age line in logarithmic space (Figure 3). It is interpreted as being inversely related to weathering rate. The power law slope, b-value, is common to all sites and indicates that there is a ubiquitous change of weathering rates through time, despite orders of magnitude differences in the rates themselves. A linear function drawn between the modern stream and the youngest terrace results in a smooth transition from linearity to power law (in logarithmic space), but is only an assumption due to lack of data in that time range (curved fine-dotted lines in Figure 3).

A Kruskal–Wallis ANOVA test shows that most terraces have statistically significant differences among their medians (Figure 4). It is rare for two terraces to have statistically indistinguishable SH_R when their numerical age errors do not overlap. The results show that SHD is ideal for relative-age dating of Pleistocene outwash plains – in the Mackenzie basin, R-value datasets that cannot be differentiated are from surfaces that are the same age. Calibrated-age dating of Holocene fluvial terraces at the other three sites is more prone to statistical 'overlap', though this is rare in the present study.

Predicted age uncertainties were computed using the 95% confidence interval of a-values and the residuals of actual age to regression age. These values yield an average 22% uncertainty with respect to terrace age. This approach to predicting age uncertainty (or more specifically equation error) is preferred in this study for its simplicity. Predicted age errors for linear regressions involving SH measurement error are discussed in full by Shakesby *et al.* (2011). Because SH_R is related to age by a power law in this study, both SH_R and age are logarithmically transformed in the regression procedure, which simultaneously transforms the errors. Thus straight-forward age error distributions using SH_R are not possible, but the double transformation reduces the increasing variability in age observed by Shakesby *et al.* (2011).

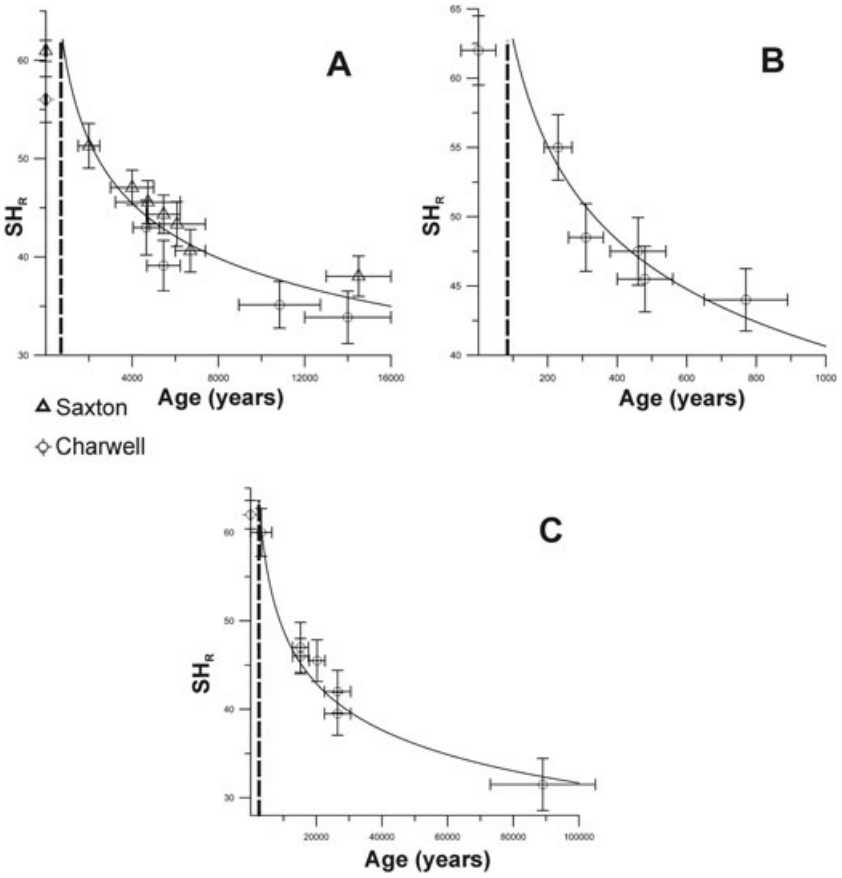

Figure 2. Individual SH_R–Age curves for (A) Saxton and Charwell River terraces; (B) Waipara River terraces; (C) Mackenzie basin outwash plains. Standard error of the median is approximated as 1 · 25 times the standard error of the mean (Hojo, 1931). Vertical asymptote is drawn through the age with a corresponding SH_R value equal to that of the modern stream.

Table IV. Statistically estimated power law constants (with 95% confidence intervals) for Equation 1

Site	*a*-Value	*b*-Value	Lower threshold of power law behaviour (SH_R; Age_{min})	R^2 to lower threshold
Saxton and Charwell	217^{+7}_{-7}	$-0{\cdot}189^{+0{\cdot}0316}_{-0{\cdot}0375}$	52; 2000	0 · 854
Waipara	150^{+3}_{-4}	$-0{\cdot}189^{+0{\cdot}0316}_{-0{\cdot}0375}$	55; 230	0 · 951
Mackenzie	281^{+5}_{-6}	$-0{\cdot}189^{+0{\cdot}0316}_{-0{\cdot}0375}$	60; 3275	0 · 9826

Note: The *p*-value (0 · 678) obtained for testing if the datasets had a common slope (*b*-value) was much higher than the critical value (0 · 05). See text for discussion.

Climate and petrographic data

The weathering rate from dissolution of a silicate mineral is often expressed with the Arrhenius equation

$$R_x = A * \exp\left(-\frac{E_a}{RT}\right) \quad (2)$$

where R_x is weathering rate, E_a is the activation energy (in kJ mol^{-1}), R is the gas constant, T is the temperature (in °K), and A is a pre-exponential factor related to mineral surface area and reactivity (Riebe *et al.*, 2004). White and Blum (1995) modified this equation to include precipitation and empirically predict chemical weathering flux at the watershed scale

$$Q_x = (c * P) * \exp\left[-\frac{E_a}{R}\left(\frac{1}{T}-\frac{1}{T_0}\right)\right] \quad (3)$$

where Q_x is the chemical weathering flux (in mol ha^{-1} yr^{-1}) of a solute, P is annual precipitation (in millimetres), T_0 is a reference temperature, and c is the slope of a linear correlation between precipitation and Q_x (set as $c = 0 \cdot 45$, after White and Blum, 1995). MAT and MAP for each month (Table III) were used to calculate ranges of Q_x for the four study sites (Figure 5A). The value of E_a was set to 60 kJ mol^{-1} which is within range reported for the dissolution of common silicate minerals (e.g. feldspars: $E_a = 45$–85 kJ mol^{-1}; White and Blum, 1995; Brady and Carroll, 1994; Riebe *et al.*, 2004) and the solution obtained for silicon dioxide (SiO_2) from a global dataset of granitoid rocks used by White and Blum (1995) ($E_a = 59 \cdot 4$ kJ mol^{-1}). A reference temperature of 288 · 15 °K (15 °C) was used, which is near the average MAT_{month} (15 · 8 °C). Because the interest in this study is comparison of *in situ* clast weathering rates, values are not normalized for watershed size and scale is arbitrary (i.e. flux and rate are interchangeable terms).

Other authors have modified Equation 3 to account for other influences on chemical weathering rate (e.g. denudation rate; Riebe *et al.*, 2004) with an additional dimensionless term on the right side of Equation 3. In Torlesse greywacke, chemical weathering occurs predominantly along intergranular boundaries, joints,

and microcracks (Watters *et al.*, 1981). Thus, to incorporate the influence of petrologic differences on the availability of fluid pathways for weathering, we multiply by the proportion of lithic fragments in the Torlesse sub-terrane (L) over a reference proportion ($L_0 = 0.5$) to obtain an adjusted chemical weathering rate (W_x) for each site

$$W_x = (c * P) * \exp\left[-\frac{E_a}{R}\left(\frac{1}{T} - \frac{1}{T_0}\right)\right] * \left(\frac{L}{L_0}\right). \quad (4)$$

Figure 5B shows the relationship of power law a-value to L for the study sites and the Cloudy Peaks test site, with the inset QFL ternary diagram showing scatter in L for the different sub-terranes. Values of W_{xmin}, W_{xmax}, $W_{xmedian}$, and W_{xavg} (the dataset mean weighted to the highest 50% of the values) are reported in Table V. Figure 5C shows a-values plotted against these measures of W_x.

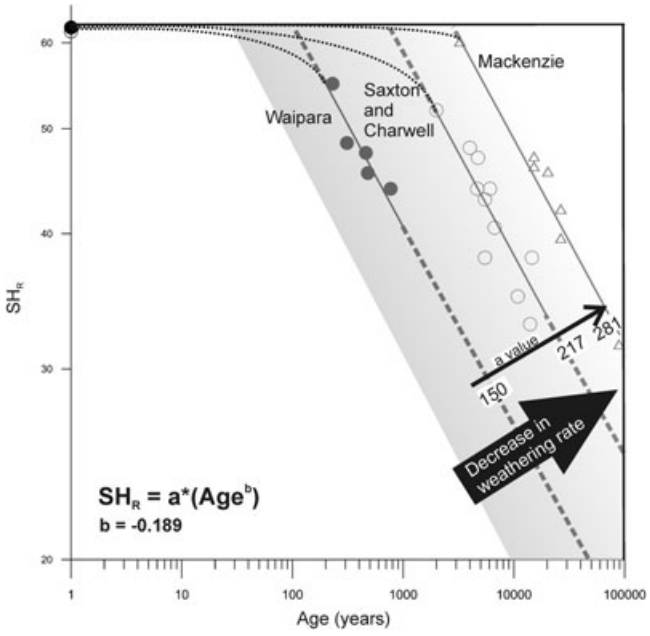

Figure 3. The SH_R–Age data on a logarithmic scale for the three curves shown in Figure 2A–2C. Dark lines (solid for known data and dashed for assumed continuation) show the maximum likelihood estimation of a common slope (b-value) for the three groups. The line position is determined by a-value in Equation 1, which increases with decreasing weathering rate. The fine-dotted lines are linear interpolations (curved when plotted on logarithmic axes) between the modern stream values and the youngest surface.

Discussion

Time dependence of SH_R

Previous studies have suggested that the mean R-value chronofunction is linear through time. Shakesby *et al.* (2011) recently confirmed this for the Holocene in relatively resistant granite boulders, but indicated that over a longer timescale (i.e. beyond the Late Glacial re-advances) weathering, and thus R-values, must inevitably reach a dynamic equilibrium. SH studies of 10^4–10^5 year timescale features have pointed towards curvilinear relationships (White *et al.*, 1998; Engel, 2007; Sánchez *et al.*, 2009; Černá and Engel, 2011), as well as some SH studies on 10^2–10^3 year timescales (McCarroll and Nesje, 1993; Betts and Latta, 2000; Awasthi *et al.*, 2005; Kellerer-Pirklbauer *et al.*, 2008). Curvilinear correlations on such short timescales could be due to comparatively small datasets, uncertainty in numerical ages, exceptionally fast weathering conditions, or coincidental, non-age related variations in rock surface hardness between study sites (Shakesby *et al.*, 2011).

Our data show that the relationship between SH_R and age is curvilinear in all instances regardless of timescale. OLS fitting of a linear regression produces reasonable results for the Waipara terraces, but even fitting of a second-order polynomial produces a higher correlation coefficient. Linear regressions at the other sites can only be obtained by excluding data from older terraces.

For numerous time-dependent weathering processes, there is laboratory and field-based evidence that the fundamental processes governing weathering follow a power law. Busenberg and Clemency (1976) noted that the kinetic dissolution of feldspars follows a power law for some stages of weathering in the laboratory. Harden (1987) found a power law relationship for the accumulation of clay content through time in soils ranging from 10 ka to 3 Ma. Taylor and Blum (1995) compared the relative proportions of cations in unweathered parent material for a glacial chronosequence and obtained a power law relationship with age. They remarked 'the explanation for the power law relationship is probably a combination of several mechanisms, including changes in mineral surface area,

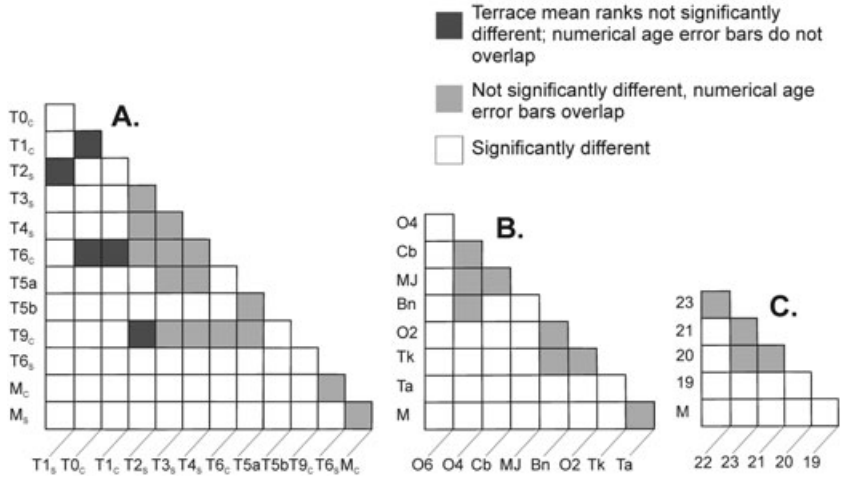

Figure 4. Matrix of Kruskal–Wallis test results. (A) Saxton and Charwell River terraces; (B) Mackenzie basin outwash plains; (C) Waipara River terraces. Subscripts S and C denote Saxton and Charwell, respectively; M, modern stream tests; O, Ohau; Cb, Clearburn1; MJ, Mt John1; Bn, Benmore; Tk, Tekapo1; Ta, Tasman Downs. See text for discussion.

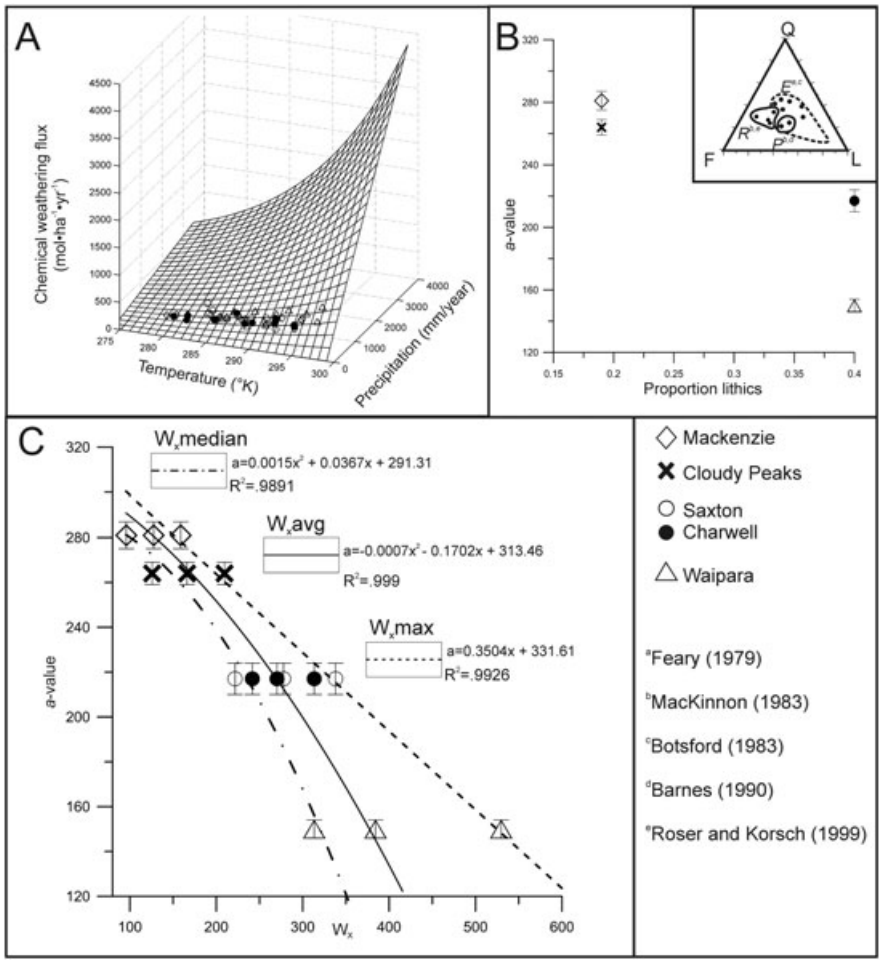

Figure 5. (A) Chemical weathering fluxes calculated by MAT_{month} and MAP_{month} for all four study sites. (B) Representative proportion of lithics in Torlesse sub-terrane versus *a*-value for the four study sites and Cloudy Peaks test site. Inset ternary diagram shows distribution of QFL percentages for *R* (Rakaia sub-terrane), *P* (Pahau sub-terrane) and *E* (Esk Head Melange sub-terrane). (C) Adjusted chemical weathering rates versus *a*-value and best-fit regressions for the four study sites. Data for the Cloudy Peaks test site is plotted but not included in the regression analysis. The key in the lower right applies to all three sub-figures.

Table V. Minimum, median, weighted average and maximum values of adjusted chemical weathering flux

Site	W_{xmin}	$W_{xmedian}$	W_{xavg}	W_{xmax}	*a*-Value
Saxton	111 · 13	221 · 72	277 · 80	337 · 99	217^{+7}_{-7}
Charwell	191 · 6	241 · 72	270 · 24	313 · 306	217^{+7}_{-7}
Waipara	166 · 93	313 · 34	384 · 24	529 · 63	150^{+3}_{-4}
Mackenzie	45 · 15	95 · 86	127 · 56	158 · 84	281^{+5}_{-6}
Cloudy Peaks	56 · 45	125 · 85	166 · 18	209 · 59	264^{+5}_{-5}

Note: The 95% confidence interval for *a*-value at Cloud Peaks is an estimate from previous results.

depletion of reactive minerals, and exhaustion of rapidly weathered minerals' (Taylor and Blum, 1995, p. 981). Simple and modified power laws are commonly used for weathering rind thickness chronofunctions in New Zealand (Chinn, 1981; Whitehouse *et al.*, 1986; Knuepfer, 1984, 1988).

Vance *et al.* (2009) reviewed the decrease in chemical weathering rate of silicate minerals with time. They show that there is a common dependence of weathering rate on time (common power law slope, *b*-value) for samples from different climates and rock-types, despite weathering rate change over several orders of magnitude (changing power law *a*-value). White and Brantley (2003) similarly reviewed weathering rates of common minerals (plagioclase, K-feldspar, biotite, and hornblende) and drew the same conclusions. These results are reflected in the current study. The trend in decreasing SH_R values with time is common among all sites, but the absolute rate varies, presumably, with small changes in petrography and/or climate. Thus, the chemical weathering of minerals provides a feasible mechanism to explain the observed power law decrease of SH_R with time as well as variations in *a*-value.

Relationship of *a*-value to climate and petrography

Modern chemical weathering rates are precipitation and temperature dependent (Equation 3; White and Blum, 1995). Figure 5A shows that chemical weathering fluxes, Q_x, are all relatively low for our study sites. More importantly, the clustering of points shows that there are only small variations in Q_x from one site to another. These variations cannot fully explain the differences in *a*-value. Since chemical weathering in Torlesse greywacke is in large part limited by the fluid pathways (e.g. intergranular boundaries) available in the rock (Watters *et al.*, 1981), differences in source terrane lithic content *L* should show a relationship with *a*-value for our sites. Figure 5B shows that there is a general negative correlation between *a*-value and increasing lithic content. Sites with the same lithic content but vastly different *a*-values (Waipara and Saxton/Charwell, Mackenzie basin and Cloudy Peaks),

however, suggests that lithic content alone does not control chemical weathering rate.

Figure 5C shows the relationship of adjusted chemical weathering rate, W_x, to *a*-value for our four study sites. The data for the Cloudy Peaks test site is plotted for comparison, but not included in determination of the regressions or correlation coefficients. The data show that the highest weathering rates at a site have a strong correlation with *a*-value; the regression is linear for W_{xmax} and a second-order polynomial for W_{xavg} and $W_{xmedian}$. The W_{xmin} does not show a useful correlation with *a*-value due to the relatively restricted range of climate fluctuations at Charwell (see Table III) and so is not plotted in Figure 5C. At Cloudy Peaks, *a*-values determined from OSL age control conform with those that would be predicted by the three separate measures of W_x. This suggests that absent independent age control, climate and petrologic information can be used to estimate *a*-value in Torlesse greywacke subterranes. We note that this empirical approach does not seek to fully describe a fundamental relationship between W_x and *a*-value. There are undoubtedly other variables, such as vegetation and site-specific chemistry differences that affect chemical weathering rates. Additionally, chemical weathering rates in paleo-climates are not addressed – it is assumed that all sites are affected equally by past climate change, though the orders of magnitude timescale differences considered here mean that this is not the case (e.g. Vance *et al.*, 2009). However, the high correlation coefficients and predictive capability of the regression equations imply that these effects are small compared to the climatic extremes and petrologic variables for which W_x accounts.

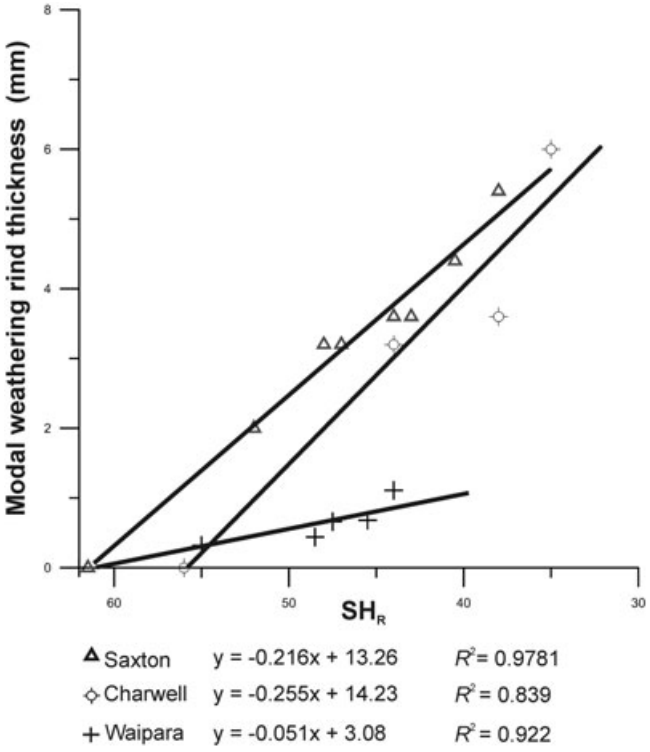

Figure 6. Relationship of SH_R to modal weathering rind thickness for the Charwell, Saxton, and Waipara River sites. References for weathering rind data are the same as for ages at respective study sites in Table I.

Relationship of chemical weathering to SH rebound

Using several geotechnical indices, Hodder and Hetherington (1991) showed that there is a quantifiable relationship between chemical weathering indices and rock strength (using SH, Shore hardness, and Point load tests) for Torlesse greywacke in New Zealand. The mechanism by which chemical alteration leads to a reduction in SH rebound requires an explanation which is considered here.

Weathering rinds are a product of chemical alteration on the outer edges of surface boulders (Whitehouse *et al.*, 1986; Oguchi and Matsukura, 1999; Birkeland and Noller, 2000). Oguchi and Matsukura (1999) found that Vickers microhardness was useful in distinguishing different zones within a weathering rind profile. Laustela *et al.* (2003) found a linear relationship between weathering rind thicknesses and SH *R*-value for rock glacier surfaces in the Swiss Alps. Likewise, SH_R and modal weathering rind thicknesses are positively co-variant at three of our study sites and best defined by linear regressions (Figure 6). This relationship indicates that an increase in weathering rind thickness occurs concurrently with a drop in mechanical strength that is measurable by the SH on timescales of ~15 ka or less. Since the slope of the SH_R-modal weathering rind thickness line changes from one area to the next, however, SH_R must be measuring another property within or on the clast.

The 'other' aspect of clast weathering could have any number of underlying chemical or physical mechanisms. Studies have outlined how rock properties that vary with surface exposure time, such as P-wave velocity (Crook and Gillespie, 1986; Sharma *et al.*, 2011), rock density (Maizels, 1989; Hodder and Hetherington, 1991; Basu *et al.*, 2007), and surface roughness (Benedict, 1985; McCarroll, 1989; André, 1996; Ericson, 2004; Gupta *et al.*, 2009) also affect SH *R*-values. Exactly how chemical weathering is coupled to each of these properties is not presently well constrained, though a decrease in reactive surface area with increasing surface roughness and/or precipitation of soft, authigenic clay minerals in or on the clast likely facilitate at least some of the reduction in SH *R*-value.

Applicability of SHD to fluvial terraces

SHD is capable of differentiating exposure-ages of surface clasts on fluvial terraces. Equation 1 and *b*-values reported in Table IV can be used to derive *a*-values for other terraces with Torlesse greywacke surface clasts and at least one age control point. An empirical relationship between *a*-value and climatic/petrologic-dependent weathering rates is suggested. At a test site, *a*-values derived using this relationship yielded similar results to solving with independent age control. Average age uncertainties of 22% of the terrace age are consistent with those of weathering rind studies (Knuepfer, 1988; 5–40%). Care should be taken in applying curves from this study to lithologies other than Torlesse greywacke, as the *b*-value and/or chronofunction may not be applicable. For other calibrated-age studies where numerical ages are not available, similar methods of adjusting constants for chemical weathering rates may be useful regardless of the form of the equation.

Conclusions

SHD is a useful calibrated-age dating technique for outwash plains and fluvial terraces. In New Zealand, SH median *R*-values are a power law function of exposure age (Equation 1, Figure 3). The power law exponent, or *b*-value, for Torlesse greywacke is the same irrespective of study site (Table IV). The power law scaling constant, or *a*-value, scales with intrinsic petrologic variations between Torlesse sub-terranes and extrinsic climatic variables, and can be directly solved for using a minimum of one age control point. Empirical relationships for predicting *a*-value without

numerical age constraints are suggested. Estimates of predicted age uncertainties (~22% of terrace age) are similar to those of weathering rind studies. Modal weathering rind thicknesses are correlated to SH *R*-values, though the changing slope of the regression from one area to the next indicates that there must be other time-related factors that influence *R*-values. If sufficient measures are taken to reduce time-independent *R*-value variability from site to site, use of SHD offers a sound alternative to numerical and other calibrated-age techniques for dating fluvial terraces over late Quaternary timescales.

Acknowledgements—This work was partially funded by a University of Canterbury Doctoral Scholarship, University of Canterbury Mason Trust grant, and New Zealand Earthquake Commission funding. The authors would like to thank the numerous landowners for allowing them access to their properties and their general interest in the work. Useful discussions with Eric Bilderback, Sam McColl, Jocelyn Campbell, Hazel Albertyn and the geomorphology groups at the University of Canterbury, Victoria University of Wellington, and Australasian Quaternary Association helped in writing this paper. Thorough reviews by Rick Shakesby and an anonymous reviewer significantly improved the presentation of the manuscript.

References

Aa AR, Sjåstad J, Sønstegaard E, Blikra LH. 2007. Chronology of Holocene rock-avalanche deposits based on Schmidt-hammer relative dating and dust stratigraphy in nearby bog deposits, Vora, inner Nordfjord, Norway. *The Holocene* **17**: 955–964. DOI. 10.1177/0959683607082411

Abdi H. 2007. The Bonferroni and Sidak corrections for multiple comparisons. In *Encyclopedia of Measurment and Statistics*, Salkind N (ed.). Sage: Thousand Oaks, CA; 1416 pp.

André MF. 1996. Rock weathering rates in arctic and subarctic environments (Abisko Mts., Swedish Lapland). *Zeitschrift für Geomorphologie* **40**: 499–517.

Amos CB, Burbank DW, Nobes DC, Read SAL. 2007. Geomorphic constraints on listric thrust faulting: Implications for active deformation in the Mackenzie Basin, South Island, New Zealand. *Journal of Geophysical Research* **112**: B03S11. DOI. 10.1029/2006JB004291

Amos CB, Burbank DW, Read SAL. 2010. Along-strike growth of the Ostler Fault, New Zealand: consequences for drainage deflection above active thrusts. *Tectonics* **29**: TC4021. DOI. 10.1029/2009TC002613

Awasthi DD, Bali R, Tewari NK. 2005. Relative dating of moraines by lichenometric and Schmidt hammer techniques in the Gangotri glacier valley, Uttarkashi District, Uttaranchal. *Special Publication of the Palaeontological Society of India* **2**: 201–206.

Aydin A. 2009. ISRM suggested method for determination of the Schmidt hammer rebound hardness: Revised version. *International Journal of Rock Mechanics and Mining Sciences* **46**: 627–634.

ASTM. 2005. Standard test method for determination of rock hardness by Rebound Hammer Method. D5873-05: 3 pp.

Barrell DJA. 2011. Quaternary glaciers of New Zealand. In *Quaternary Glaciations – Extent and Chronology: A Closer Look*, Ehlers J, Gibbard PL, Hughes PD (eds), Developments in Quaternary Science 15. Elsevier: Amsterdam; 1047–1064.

Barrell DJA, Andersen BG, Denton GH. 2011. *Glacial Geomorphology of the Central South Island, New Zealand*, GNS Science monograph 27. GNS Science: Lower Hutt.

Barrell DJA, Cox S. 2003. Southern Alps tectonics and Quaternary geology. In *Geological Society of New Zealand Annual Conference Field Trip Guide FT6*, Cox S, Lyttle BS (comp.), Geological Society of New Zealand Miscellaneous Publication 116B. Geological Society: Christchurch; 40 pp.

Barnes PM. 1990. Provenance of Cretaceous accretionary wedge sediments: the Mangapokia Formation, Wairarapa, New Zealand. *New Zealand Journal of Geology and Geophysics* **33**: 125–135.

Basu A, Celestino TB, Bortolucci AA. 2007. Predicting weathering grades by Schmidt hammer test: an investigation on granitic rock materials from Southeastern Brazil. *Proceedings of the 11th Congress of the International Society for Rock Mechanics (ISRM)*, Lisbon, Portugal; 385–390.

Benedict JB. 1985. *Arapaho Pass, Glacial Geology and Archaeology at the Crest of the Colorado Front Range*, Research Report no. 3. Center for Mountain Arachaeology: Ward, CO; 197 pp.

Betts MW, Latta MA. 2000. Rock surface hardness as an indication of exposure age: an archaeological application of the Schmidt hammer. *Archaeometry* **42**: 209–223.

Birkeland PW, Noller JS. 2000. Rock and mineral weathering. In *Quaternary Geochronology: Methods and Applications*, Noller JS, Sowers JM, Lettis WR (eds) American Geophysical Union: Washington, DC; 293–312.

Botsford JW. 1983. The Esk Head Melange in the Eske Head/Okuku Area, North Canterbury. Unpublished MSc thesis, University of Canterbury, New Zealand; 247 pp.

Brady PV, Carroll SA. 1994. Direct effects of CO_2 and T on silicate weathering: possible implications for climate control. *Geochimica et Cosmochimica Acta* **58**: 1853–1856.

Bull WL. 1990. Stream-terrace genesis: implications for soil development. *Geomorphology* **3**: 351–367.

Bull WL, Knuepfer PLK. 1987. Adjustments by the Charwell River, New Zealand, to uplift and climatic changes. *Geomorphology* **1**: 15–32.

Busenberg E, Clemency CV. 1976. The dissolution kinetics of feldspars at 25 °C and 1 atm CO_2 partial pressure. *Geochimica et Cosmochimica Acta* **40**: 41–49.

Campbell JK, Nicol A, Howard ME. 2003. Long-term changes to river regimes prior to late Holocene coseismic faulting, Canterbury, New Zealand. *Journal of Geodynamics* **36**: 147–168.

Chinn TJH. 1981. Use of rock weathering-rind thickness for Holocene numerical age-dating in New Zealand. *Arctic and Alpine Research* **13**: 33–45.

Černá B, Engel Z. 2011. Surface and subsurface Schmidt hammer rebound value variation for a granite outcrop. *Earth Surface Processes and Landforms* **36**: 170–179.

Challis GA. 1966. Cretaceous stratigraphy and structure of the Lookout area, Awatere Valley. *Transactions of the Royal Society of New Zealand* **4**: 119–137.

Crook R, Gillespie AR. 1986. Weathering rates in granitic boulders measured by P-wave speeds. In *Rates of Chemical Weathering of Rocks and Minerals*, Colman SM, Dethier DP (eds). Academic Press: Orlando, FL; 395–417.

Day MJ. 1980. Rock hardness: field assessment and geomorphic importance. *The Professional Geographer* **32**: 72–81.

Day MJ, Goudie AS. 1977. Field assessment of rock hardness using the Schmidt test hammer. *British Geomorphology Research Group Technical Bulletin* **18**: 19–29.

Demirdag S, Yavuz H, Altindag R. 2009. The effect of sample size on Schmidt rebound hardness value of rocks. *International Journal of Rock Mechanics and Mining Sciences* **46**: 725–730.

Engel Z. 2007. Measurement and age assignment of intact rock strength in the Krkonoše Mountains, Czech Republic. *Zeitschrift für Geomorphologie* **51**(Suppl. 1): 69–80.

Ericson K. 2004. Geormorphological surfaces of different age and origin in granite landscapes: an evaluation of the Schmidt hammer test. *Earth Surface Processes and Landforms* **29**: 495–509. DOI. 10.1002/esp.1048

Feary DA. 1979. Geology of the Urewera Greywacke in Waioeka Gorge, Raukumara Peninsula, New Zealand. *New Zealand Journal of Geology and Geophysics* **22**: 693–708.

Goudie AS. 2006. The Schmidt hammer in geomorphological research. *Progress in Physical Geography* **30**: 703–718. DOI. 10.1177/0309133306071954

Gupta V, Sharma R, Sah MP. 2009. An evaluation of surface hardness of natural and modified rocks using Schmidt hammer: study from northwestern Himalaya, India. *Geografiska Annaler* **91**: 179–188.

Harden JW. 1987. Soils developed in granitic alluvium near Merced, California. US Geological Survey Bulletin. 1590-A: 65 pp.

Hodder APW, Hetherington JR. 1991. A quantiative study of the weathering of greywacke. *Engineering Geology* **31**: 353–368.

Hojo T. 1931. Distribution of the median, quartiles and interquartile distance in samples from a normal population. *Biometrika* **23**: 315–360.

Kellerer-Pirklbauer A, Wangensteen B, Farbrot H, Etzelmüller B. 2008. Relative surface age-dating of rock glacier systems near Hólar,

Hjaltadalur, northern Iceland. *Journal of Quaternary Science* **23**: 137–151. DOI. 10.1002/jqs.1117

Knuepfer PLK. 1984. Tectonic Geomorphology and Present-day Tectonics of the Alpine Shear System, South Island, New Zealand. Unpublished PhD Thesis, University of Arizona, Tucson, AZ; 489 pp.

Knuepfer PLK. 1988. Estimating ages of late Quaternary stream terraces from analysis of weathering rinds and soils. *GSA Bulletin* **100**: 1224–1236.

Kruskal WH, Wallis WA. 1952. Use of ranks in one-criterion variance analysis. *Journal of the American Statistical Association* **47**: 583–621.

Laustela M, Egli M, Frauenfelder R, Kääb A, Maisch M, Haeberli W. 2003. Weathering rind measurements and relative age dating of rockglacier surfaces in crystalline regions of the Eastern Swiss Alps. *Permafrost*: *Proceedings of the Eighth International Conference on Permafrost, July 2003*, Phillips M, Springman S, Arenson L (eds), Zurich; 627–632.

MacKinnon TC. 1983. Origin of the Torlesse terrane and coeval rocks, South Island, New Zealand. *Geological Society of America Bulletin* **93**: 625–634.

Maizels J. 1989. Differentiation of late Pleistocene terrace outwash deposits using geomorphic criteria: Tekapo valley, South Island, New Zealand. *New Zealand Journal of Geology and Geophysics* **32**: 225–241.

Mason DPM, Little TA, Van Dissen RJ. 2006. Rates of active faulting during late Quaternary fluvial terrace formation at the Saxton River, Awatere Fault, New Zealand. *GSA Bulletin* **118**(11/12): 1431–1446. DOI. 10.1130/B25961.1

Matthews JA, Owen G. 2010. Schmidt hammer exposure-age dating: developing linear age-calibration curves using Holocene bedrock surfaces from the Jotunheimen-Jostedalsbreen regions of southern Norway. *Boreas* **39**: 105–115. DOI. 10.1111/j.1502-3885.2009.00107.x

Matthews JA, Shakesby RA. 1984. The status of the 'Little Ice Age' in southern Norway: relative-age dating of neoglacial moraines with Schmidt hammer and lichenometry. *Boreas* **13**: 333–346.

Matthews JA, Winkler S. 2011. Schmidt-hammer exposure-age dating (SHD): application to early Holocene moraines and a reappraisal of the reliability of terrestrial cosmogenic-nuclide dating (TCND) at Austanbotnbreen, Jotunheimen, Norway. *Boreas* **40**: 256–270.

McCalpin JP. 1996. Tectonic geomorphology and Holocene paleoseismicity of the Molesworth section of the Awatere fault, South Island, New Zealand. *New Zealand Journal of Geology and Geophysics* **39**: 33–50.

McCarroll D. 1987. The Schmidt hammer in geomorphology: five sources of instrument error. *British Geomorphology Research Group Technical Bulletin* **36**: 16–27.

McCarroll D. 1989. Potential limitations of the Schmidt hammer for relative-age dating: field tests on Neoglacial moraines, Jotunheimen, southern Norway. *Arctic and Alpine Research* **21**: 268–275.

McCarroll D. 1991a. The Schmidt hammer, weathering and rock surface roughness. *Earth Surface Processes and Landforms* **16**: 477–480.

McCarroll D. 1991b. The age and origin of Neoglacial moraines in Jotunheimen, southern Norway: new evidence from weathering-based data. *Boreas* **20**: 283–295.

McCarroll D. 1991c. Relative-age dating of inorganic deposits: the need for a more critical approach. *The Holocene* **1**: 174–180.

McCarroll D. 1994. The Schmidt hammer as a measure of degree of rock surface weathering and terrain age. In *Dating in Exposed and Surface Contexts*. Beck C (ed.). University of New Mexico Press: Albuquerque, NM; 29–46.

McCarroll D, Nesje A. 1993. The vertical extent of ice sheets in Sunnmøre, western Norway: measuring degree of rock surface weathering. *Boreas* **22**: 255–265.

McSaveney M. 1992. *A Manual for Weathering-rind Dating of Grey Sandstones of the Torlesse Supergroup, New Zealand*, GNS Science Report 92/04. Institute of Geological and Nuclear Sciences: Lower Hutt; 52 pp.

Molnar P, Brown ET, Burchfiel BC, Qidong D, Xianyue F, Jun L, Raisbeck GM, Jianbang S, Zhangming W, Yiuo F, Huichuan Y. 1994. Quaternary climate change and the formation of river terraces across growing anticlines on the North Flank of the Tien Shan, China. *Journal of Geology* **102**: 583–602.

Nesje A, Blikra LH, Anda E. 1994a. Dating rockfall-avalanche deposits from degree of weathering by Schmidt-hammer tests: a study from Norangsdalen, Sunnmøre, Norway. *Norsk Geologisk Tidsskrift* **74**: 108–113.

Nesje A, McCarroll D, Dahl SO. 1994b. Degree of rock surface weathering as an indicator of ice-sheet thickness along an east-west transect across southern Norway. *Journal of Quaternary Sciences* **9**: 337–347.

Nicholas JW, Butler DR. 1996. Application of relative-age dating techniques on rock glaciers of the La Sal Mountains, Utah: an interpretation of Holocene paleoclimates. *Geografiska Annaler* **78**: 1–18.

Nicol A, Campbell JK. 2001. The impact of episodic fault-related folding on late Holocene degradation terraces along Waipara River, New Zealand. *New Zealand Journal of Geology and Geophysics* **44**: 145–156. DOI. 10.1080/00288306.2001.9514931

Niedzielski T, Migoń P, Placek A. 2009. A minimum sample size required from Schmidt hammer measurements. *Earth Surface Processes and Landforms* **34**: 1713–1725. DOI. 10.1002/esp.1851

Norton DA. 1985. A multivariate technique for estimating New Zealand temperature normals. *Weather and Climate* **5**: 64–74.

Oguchi CT, Matsukura Y. 1999. Effect of porosity on the increase in weathering-rind thickness of andesite gravel. *Engineering Geology* **55**: 77–89.

Ozbek A, Gul M. 2011. Variation of Schmidt hammer rebound values depending on bed thickness and discontinuity surfaces. *Scientific Research and Essays* **6**: 2201–2211.

Proceq SA. 2004. *Concrete Test Hammer – Operating Instructions*. Proceq SA: Schwerzenbach; 14 pp.

Read SAL, Richards LR, Perrin ND. 1999. Applicability of the Hoek–Brown failure criterion to New Zealand greywacke rocks. *Proceedings 9th International Congress on Rock Mechanics, 1999*, Paris; **2**: 655–660.

Riebe CS, Kirchner JW, Finkel RC. 2004. Erosional and climatic effects on long-term chemical weathering rates in granitic landscapes spanning diverse climatic regimes. *Earth and Planetary Science Letters* **224**: 547–562.

Rode M, Kellerer-Pirklbauer A. 2011. Schmidt-hammer exposure-age dating (SHD) of rock glaciers in the Schöderkogel-Eisenhut area, Schladminger Tauern Range, Austria. *The Holocene* **22**: 761–771. DOI. 10.1177095968361143041O

Roser BP, Korsch RJ. 1999. Geochemical characterization, evolution and source of a Mesozoic accretionary wedge: the Torlesse terrane, New Zealand. *Geology Magazine* **136**: 493–512.

Sánchez J, Mosquera DF, Romaní JRV. 2009. Assessing the age-weathering correspondence of cosmogenic ^{21}Ne dated Pleistocene surfaces by the Schmidt hammer. *Earth Surface Processes and Landforms* **34**: 1121–1125. DOI. 10.1002/esp.1802

Schaefer JM, Denton GH, Kaplan M, Putnam A, Finkel RC, Barrell DJA, Andersen BG, Schwartz R, Mackintosh A, Chinn T, Schlüchter C. 2009. High frequency Holocene glacier fluctuations in New Zealand differ from the northern signature. *Science* **324**: 622–625. DOI. 10.1126/science.1169312

Schmidt E. 1951. A non-destructive concrete tester. *Concrete* **59**: 34–35.

Shakesby RA, Matthews JA, Karlén W, Los SO. 2011. The Schmidt hammer as a Holocene calibrated-age dating technique: testing the form of the *R*-value–age relationship and defining the predicted-age errors. *The Holocene* **21**: 615–628. DOI. 10.1177/0959683610391322

Shakesby RA, Matthews JA, Owen G. 2006. The Schmidt hammer as a relative-age dating tool and its potential for calibrated-age dating in Holocene glaciated environments. *Quaternary Science Reviews* **25**: 2846–2867.

Sharma PK, Khandelwal M, Singh TN. 2011. A correlation between Schmidt hammer rebound numbers with impact strength, slake durability index and P-wave velocity. *International Journal of Earth Science* **100**: 189–195. DOI. 10.1007/s00531-009-0506-5

Sidak Z. 1967. Rectangular confidence regions for the means of multivariate normal distributions. *Journal of the American Statistical Association* **62**: 626–633.

Suggate RP. 1958. Geology of the Clarence Valley from Gore Stream to Bluff Hill. *Transactions of the Royal Society of New Zealand* **85**: 397–408.

Sumner P, Nel W. 2002. The effect of rock moisture on Schmidt hammer rebound: tests on rock samples from Marion Island and South

Africa. *Earth Surface Processes and Landforms* **27**: 1137–1142. DOI. 10.1002/esp.402

Taylor A, Blum JD. 1995. Relation between soil age and silicate weathering rates determined from the chemical evolution of a glacial chronosequence. *Geology* **23**: 979–982.

Walker M. 2005. *Quaternary Dating Methods*. Wiley: Chichester; 286 pp.

Warton DI, Wright IJ, Falster DS, Westoby M. 2006. Bivariate line-fitting methods for allometry. *Biological Reviews* **81**: 259–291. DOI. 10.1017/S1464793106007007

Watters WA, Soong CWR, Riddolls BW. 1981. Weathering of greywacke sandstone, Wellington, New Zealand. *Proceedings of the International Symposium on Weak Rock, 1981*, Akai K, Hayashi M, Nishimatsu Y (eds), Tokyo; **1**: 179–184.

White AF, Blum AE. 1995. Effects of climate on chemical weathering in watersheds. *Geochimica et Cosmochimica Acta* **59**: 1729–1747.

White AF, Brantley SL. 2003. The effect of time on the weathering of silicate minerals: why do weathering rates differ in the laboratory and the field? *Chemical Geology* **202**: 479–506.

White K, Bryant R, Drake N. 1998. Techniques for measuring rock weathering: application to a dated fan segment sequence in southern Tunisia. *Earth Surface Processes and Landforms* **23**: 1031–1043.

Whitehouse IE, McSaveney MJ, Knuepfer PLK, Chinn TJ. 1986. Growth of weathering rinds on Torlesse sandstone, Southern Alps, New Zealand. In *Rates of Chemical Weathering of Rocks and Minerals*, Colman SM, Dethier DP (eds). Academic Press: Orlando, FL; 419–435.

Williams RBG, Robinson DA. 1983. The effect of surface texture on the determination of the surface hardness of rock using Schmidt Hammer. *Earth Surface Processes and Landforms* **8**: 289–292.

Winkler S. 2005. The Schmidt hammer as a relative-age dating technique: potential limitations of its application on Holocene moraines in Mt. Cook National Park, Southern Alps, New Zealand. *New Zealand Journal of Geology and Geophysics* **48**: 105–116. DOI. 0028–8306/05/4801–0105

Winkler S. 2009. First attempt to combine terrestrial cosmogenic nuclide (^{10}Be) and Schmidt hammer relative-age dating: Strauchon Glacier, Southern Alps, New Zealand. *Central European Journal of Geosciences* **1**: 274–290.

Vance D, Teagle DAH, Foster GL. 2009. Varying Quaternary chemical weathering fluxes and imbalances in marine geochemical budgets. *Nature Letters* **458**: 493–496.

Velbel MA. 1990. Influence of temperature and mineral surface characteristics on feldspar weathering rates in natural and artificial systems: a first approximation. *Water Resources Research* **26**: 3049–3053.

Viles H, Goudie A, Grab S, Lalley J. 2011. The use of the Schmidt Hammer and Equotip for rock hardness assessment in geomorphology: a comparative analysis. *Earth Surface Processes and Landforms* **36**: 320–333.

